DENTAL MATERIALS 34 (2018) e182–e195

Available online at www.sciencedirect.com

ScienceDirect

journal homepage: www.intl.elsevierhealth.com/journals/dema

Antibacterial photocatalytic activity of different crystalline TiO_2 phases in oral multispecies biofilm

Heloisa N. Pantaroto[a], *Antonio P. Ricomini-Filho*[b], *Martinna M. Bertolini*[c], *José Humberto Dias da Silva*[d], *Nilton F. Azevedo Neto*[d], *Cortino Sukotjo*[e], *Elidiane C. Rangel*[f], *Valentim A.R. Barão*[a,*]

[a] *Department of Prosthodontics and Periodontology, Piracicaba Dental School, Univ. of Campinas (UNICAMP), Av. Limeira, 901, Piracicaba, São Paulo 13414-903, Brazil*

[b] *Department of Physiological Science, Piracicaba Dental School, University of Campinas (UNICAMP), Av. Limeira, 901, Piracicaba, São Paulo 13414-903, Brazil*

[c] *Oral Health and Diagnostic Sciences Department, Division of Periodontology, University of Connecticut, School of Dental Medicine, 263 Farmington Avenue, Farmington, CT 06030, USA*

[d] *Department of Physics, Univ Estadual Paulista (UNESP), Av. Eng. Luís Edmundo C. Coube, 14-01, Bauru, São Paulo 17033-360, Brazil*

[e] *Department of Restorative Dentistry, Univ of Illinois at Chicago (UIC), College of Dentistry, 801 S. Paulina, Chicago, IL 60612, USA*

[f] *Laboratory of Technological Plasmas, Engineering College, Univ Estadual Paulista (UNESP), Av. Três de Março, 511, Sorocaba, São Paulo 18087-180, Brazil*

ARTICLE INFO

Article history:
Received 13 September 2017
Received in revised form
23 March 2018
Accepted 23 March 2018

Keywords:
Titanium oxide
Sputtering
Phototherapy
Bacteria
Biofilms
Dental implants

ABSTRACT

Objective. Titanium dioxide (TiO_2) incorporation in biomaterials is a promising technology due to its photocatalytic and antibacterial activities. However, the antibacterial potential of different TiO_2 crystalline structures on a multispecies oral biofilm remains unknown. We hypothesized that the different crystalline TiO_2 phases present different photocatalytic and antibacterial activities.

Methods. Three crystalline TiO_2 films were deposited by magnetron sputtering on commercially pure titanium (cpTi), in order to obtain four groups: (1) machined cpTi (control); (2) A-TiO_2 (anatase); (3) M-TiO_2 (mixture of anatase and rutile); (4) R-TiO_2 (rutile). The morphology, crystalline phase, chemical composition, hardness, elastic modulus and surface free energy of the surfaces were evaluated. The photocatalytic potential was assessed by methylene blue degradation assay. The antibacterial activity was evaluated on relevant oral bacteria, by using a multispecies biofilm (*Streptococcus sanguinis*, *Actinomyces naeslundii* and *Fusobacterium nucleatum*) formed on the treated titanium surfaces (16.5 h) followed by UV-A light exposure (1 h) to generate reactive oxygen species production.

Results. All TiO_2 films presented around 300 nm thickness and improved the hardness and elastic modulus of cpTi surfaces ($p < 0.05$). A-TiO_2 and M-TiO_2 films presented superior

* *Corresponding author at*: Av. Limeira, 901, Piracicaba, SP 13414-903, Brazil.
E-mail addresses: helopantaroto@hotmail.com (H.N. Pantaroto), pedroricomini@gmail.com (A.P. Ricomini-Filho), bertolini@uchc.edu (M.M. Bertolini), jhdsilva@fc.unesp.br (J.H. Dias da Silva), nilton@fc.unesp.br (N.F. Azevedo Neto), csukotjo@uic.edu (C. Sukotjo), elidiane@sorocaba.unesp.br (E.C. Rangel), vbarao@unicamp.br (V.A.R. Barão).

https://doi.org/10.1016/j.dental.2018.03.011

photocatalytic activity than R-TiO_2 ($p < 0.05$). M-TiO_2 revealed the greatest antibacterial activity followed by A-TiO_2 (≈99.9% and 99% of bacterial reduction, respectively) ($p < 0.001$ vs. control). R-TiO_2 had no antibacterial activity ($p > 0.05$ vs. control).

Significance. This study brings new insights on the development of extra oral protocols for the photocatalytic activity of TiO_2 in oral biofilm-associated disease. Anatase and mixture-TiO_2 showed antibacterial activity on this oral bacterial biofilm, being promising surface coatings for dental implant components.

1. Introduction

Despite the evidence of excellent dental implant therapy results, peri-implant mucositis and peri-implantitis disease can still occur if pathogenic bacteria accumulate on the implant surface and its components, such as abutments [1]. While peri-implant mucositis is characterized by inflammatory soft tissue infiltrate around the implant, peri-implantitis presents signs of inflammation combined with bone loss around osseointegrated implants [2]. According to a recent meta-analysis study, the overall prevalence of peri-implant mucosistis can be as high as 43%, while peri-implantitis prevalence is around 22% [3]. Therefore, the importance of preventing biofilm formation on implant structures and dental implant components is highlighted, as mucositis can potentially progressing into peri-implantitis if left untreated.

Once dental implant component, such as abutments are exposed in the oral cavity, their surfaces are immediately covered with an acquired pellicle and instantly subjected to bacterial colonization [4]. The genera *Actinomyces* and *Streptococcus* are the main initial colonizers in oral cavity and a common secondary colonizer associated with peri-implantitis is *Fusobacterium* spp. [5,6]. This bacterial colonization is directly influenced by the materials surface properties including chemical composition, surface roughness and surface free energy [7]. Hence, the development of films onto dental implant abutments and dental implant surfaces have been investigated as a possible approach to make their surfaces less prone to biofilm colonization, helping the long-term success of implant therapy [8].

For this reason, in order to reduce bacterial colonization to dental implants and their components, some photocatalytic compounds, such as titanium dioxide (TiO_2), have been incorporated to their surfaces [9–13]. When photocatalyzed TiO_2 produces reactive oxygen species (ROS) [14] that promotes the degradation of bacterial membranes, therefore presenting an antibacterial effect [15]. However, this process depends on the band gap of the materials, which can be different, depending on the crystalline form. The TiO_2 occurs in two main crystalline forms: anatase and rutile [16]. The band gap of TiO_2 corresponds to about 3.2 eV for anatase and around 3.0 eV for rutile and it can only absorb ultraviolet light (UV) (≤400 nm) [17,18]. Among UV light sources, the UV-A ($\lambda = 315–400$ nm) has been used in some studies [15,19–21] as the longer wavelength is less harmful to the host cells [15,22,23].

Several methods are used for TiO_2 deposition on biomaterials such as sol–gel [24,25], spin-coating [12,26], anodization [9,10,27], atomic layer deposition [28] and magnetron sputtering [11,13,29–31]. Magnetron sputtering is a extensively used method as it produces films with greater adhesion, hardness and hydrophilicity [19,30,32,33], and it is also able to generate isolated phases of anatase and rutile [34]. Therefore, it would be of great value aggregate the qualities of sputtered films with the promising antibacterial effect of TiO_2.

Even though the antibacterial effect of TiO_2 has been investigated in some previous studies using different deposition methods [8,11,12,35,36] it is difficult to perform comparisons between them [35] and, consequently, obtain consistent conclusions about the TiO_2 application. This is due to the high variability in the test conditions used for different studies. In one hand, studies reported that TiO_2 has an antibacterial effect [8–10,27,28,37–40], while on the other hand, different studies revealed no influence on early biofilm formation [9,36], highlighting the need for further studies.

Furthermore, there is no study that has investigated the TiO_2 photocatalytic and antibacterial activities on a multispecies biofilm composed by 3 peri-implantitis specific microorganisms, while simulating the oral environment in the implant abutment area, with a previous acquired saliva pellicle, which is a strong point about our study, since it resembles the *in vivo* situation. In addition, no study has correlated the bacterial adhesion on different crystalline phases of TiO_2 films during the light exposure, which is critically important, since different TiO_2 phases present different effects.

Therefore, in this study we developed TiO_2 films with different crystalline phases (anatase, rutile and a mixture of both) onto commercially pure titanium (cpTi) surfaces using magnetron sputtering, aiming to evaluate which crystalline phase would be able to produce more ROS after UV-A light activation, and then leading to greater biofilm reduction. Our hypothesis is that each crystalline phase will have a different antibacterial effect against the *in vitro* biofilm tested. For this, the physical–chemical, photocatalytic degradation and antibacterial properties of these titanium coatings were analyzed by using a periimplantitis-associated oral multispecies biofilm model composed of *Streptococcus sanguinis*, *Actinomyces naeslundii* and *Fusobacterium nucleatum*.

2. Materials and methods

2.1. Experimental design

CpTi discs (grade II, American Society for Testing of Material) (MacMaster Carr), 10 mm diameter and 2 mm thickness, were

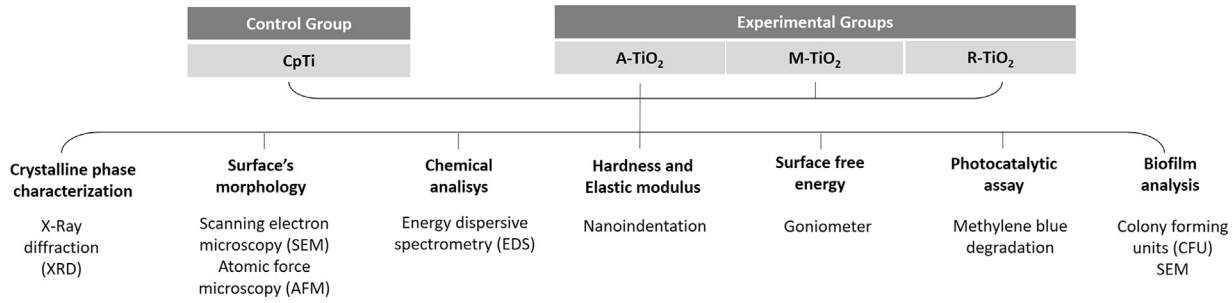

Fig. 1 – Experimental design of the study.

randomly divided and submitted to radiofrequency (RF) magnetron sputtering treatment to obtain TiO_2 films composed of anatase (A-TiO_2), rutile (R-TiO_2) or mixture (anatase + rutile) (M-TiO_2) of crystalline structures (experimental groups). The control group (cpTi) was not treated. The crystalline phase analysis (n = 1), morphology (n = 1), chemical composition (n = 1), hardness (n = 1) and surface free energy (n = 5) of the films were assessed. The photocatalytic activity was evaluated using the methylene blue degradation technique (n = 3). For the microbial assay, a multispecies biofilm composed of *S. sanguinis*, *A. naeslundii* and *F. nucleatum* was developed onto discs for 16.5 h in a modified fluid universal medium (mFUM). Afterwards, the early biofilm was exposed to a customized UV-A light apparatus for 1 h to photocatalyze TiO_2 surfaces and produce ROS. Immediately after that, the number of colony forming units (CFU) (n = 6) was measured for each specie and total bacteria, as well as the organization of the remaining biofilm was assessed by scanning electron microscopy (SEM) (n = 1) (Fig. 1).

2.2. Preparation of titanium discs and surface film

CpTi discs were polished using sequential SiC grinding papers (#320, #400 and #600) (Carbimet 2, Buehler) in an automatic polisher (EcoMet/AutoMet 250 Pro, Buehler). Samples were ultrasonically cleaned in deionized water (10 min) and degreased in 70% propanol (10 min) (Sigma-Aldrich) and hot air dried [41].

TiO_2 films were deposited on cpTi discs substrate by RF magnetron sputtering in a Kurt J. Lesker sputtering chamber (model KJL—System I) using a Ti-metal target (99.999%) (Kurt J. Lesker) and Ar + O_2 mixture. Before each deposition, the target was sputtered with Ar for 10 min to ensure that the target was cleaned during the film growth process [42]. The main deposition parameters of the films were based on previous studies [34,43] and the constant and variable parameters are summarized in Table 1. The sputtered samples were individually stored on dust free small bags before the surface analysis.

2.3. Surface analyses

The surface analyses were performed to fully characterize and to better understand the differences among the surface treatments, since not all of them direct correlates with the biofilm formation itself.

2.3.1. Energy dispersive spectroscopy (EDS)

The elemental composition (% atomic) was obtained by EDS (JEOL JSM-6010LA) (n = 1) in three different areas of each surface [44].

2.3.2. X-ray diffraction

For assessment of the surface crystalline phases, an X-ray diffraction (XRD) (Rigaku-Ultima 2000+) was employed using Cu-K$\alpha - \lambda = 1.54056$ Å in a radiation operating at 40 kV and 20 mA at a continuous speed of 0.02° per second in a fixed angle 2.5° and a scan range from 15° to 80° (n = 1) [44].

2.3.3. Scanning electron microscopy (SEM) and atomic force microscopy (AFM)

Surface morphology was analyzed by SEM (JEOL IT-300/2015) (n = 1). The AFM micrographs were measured in a 5 μm × 5 μm scan area in a tapping mode with a constant force of 42 N/m and frequency of 320 kHz by an AFM (Park System-NX-10). Roughness average (Ra) values were obtained in three different areas (n = 1), and the total surface area of the disc was estimated using specific software (Gwyddion v 2.37; GNU General Public License).

2.3.4. Measurement of TiO_2 film thickness

For the TiO_2 film thickness measurement, the deposition was performed in half of an amorphous silica (a-SiO_2) substrate (n = 1), and the step between the untreated and treated area was measured in three different areas by a profilometer (Dektak 150-d; Veeco).

2.3.5. Hardness and elastic modulus

The hardness and elastic modulus were determined by nanoindentation analysis performed in a Hysitron Triboindenter system using a ten-step partial unloads function (200–5000 μN) applied by a Berkovick diamond indenter. For each load, ten indentations were performed (n = 1) [45].

2.3.6. Surface free energy

The surface free energy (n = 5) was analyzed in a goniometer (ramé-Hart 10000; ramé-hart instrument co.) using the sessile drop (15 μL) method through the Owens–Wendt approach. The Owens–Wendt method (also known as the Kaelble–Owens–Wendt method) consists in determining components of dispersion and polar SFE on the basis of the Bethelot hypothesis which claims that interactions between molecules of two substances, present in their surface layer,

Table 1 – Deposition parameters of TiO_2 films prepared by RF magnetron sputtering.

Constant parameters

Target – metallic Ti (99.999%) – 7.62 cm of diameter and 0.6 cm thickness
Reflected RF power — 1 to 5 W depending on deposition
Target to substrate distance: 70 mm
Substrates — cpTi discs
Residual pressure of the sputtering chamber was smaller than 1×10^{-6} Torr.
Ar flux — 40 SCCM

Variable parameters

Crystalline phase	O_2 flux (SCCM)	Pressure (Torr)	RF Power (W)	Total time deposition (min)	Heater temp (°C)	Film temp[a] (°C)
Anatase	1	3.0×10^{-2}	120	900	200	120
Mixture	1	1.2×10^{-2}	240	660	400	288
Rutile	4	2.3×10^{-2}	280	420	600	504

[a] The temperature on the substrate surfaces was measured by a K type (Cromel/Alumel) thermocouple.

are equal to the geometric mean of intermolecular interactions within each substance. To determine the surface free energy, two measured liquids (water and diiodomethane) whose surface tension and polar and dispersion components of surface free energy are known were used: The water (polar component—51 mJ/m^2 with total surface free energy 72.8 mJ/m^2) and the diiodomethane (dispersive component-polar—2.4 mJ/m^2, dispersive—48.6 mJ/m^2). Their contact angles were then calculated using the ramé-hart DROP image Standard software (ramé-hart instrument co.) [46].

2.4. *Photocatalytic degradation assay*

The main reason to perform this assay was to establish the ideal UV-A light exposure time and to ensure the greatest photocatalytic potential for the studied surfaces. Furthermore, this assay was also accomplished to investigate the behavior of the surfaces in UV-A light absence. Therefore, the methylene blue (MB) ISO technique was used to investigate the photocatalytic degradation activity of the TiO_2 films [16,47]. The specimens previous sterilized by gamma radiation (14.50 ± 0.05 kGy) [48] were soaked in 2 mL of standard MB (P.A.-C.I. 52.015, Synth) solution (10 μmol/L) in dark conditions (foil wrapped) for 12 h prior to the test [40] to eliminate reduction in the concentration of MB via absorption by the specimens. Subsequently, discs were placed in a 24-well polystyrene cell culture plate with 2 mL of fresh MB solution (10 μmol/L) in each well. The control (cpTi) and experimental (A-TiO_2, M-TiO_2 and R-TiO_2) groups were submitted to two experiments (n = 3 per group), one in the presence of light and another under dark conditions (foil wrapped). The light source used was UV-A 2 × 15 W (λ = 350 nm and intensity = 1.62 mW/cm^2) (F15T8/Black Light Silvania) perpendicularly fixed 7 cm apart from the discs [19] in a customized apparatus.

The degradation of the MB as a function of irradiation time (15, 30, 60, 90, 120, 180 and 240 min) was measured spectrophotometrically (DU 800 — Beckman Coulter) by sampling the solution and returning the sample after the measurement of the solution's absorbance at 664 nm [47]. The photocatalytic activity of the TiO_2 films was calculated using Eq. (1):

$$\text{Photocatalytic activity}(\%) = [(c_o - c)/c_o] \times [c_1/c_o] \times 100 \quad (1)$$

where c_o is the concentration of the test solution of MB before irradiation, c is the concentration of MB after UV irradiation, and c_1 is the concentration of MB after the pre-adsorption test [16].

2.5. *Microbiological assay*

2.5.1. *Pilot study*

A pilot study was performed to test the viability of bacteria cells at different UV-A light exposure times (0, 1, 2, 3 and 4 h), and to determine the ideal light exposure time to bacterial live. For this, only control surfaces (CpTi) were included to avoid confusing dead cell results regarding UV-A light or TiO_2 films. This study was performed under the same conditions described below.

2.5.2. *Experimental study*

The control groups: i. CpTi discs in dark condition; ii. CpTi discs in light presence, and test groups: iii. A-TiO_2; iv. M-TiO_2 and v. R-TiO_2 were submitted to three independent microbiological assays (n = 6) (Fig. 2). Only control (CpTi) group was investigated in both dark and light conditions, because of two factors:

1. No activity of TiO_2 in dark conditions was observed on MB degradation test.
2. It certifies that the dead cells on the other groups were not a result of UV-A light exposure.

2.5.3. *Acquired pellicle formation*

This study was approved by the Local Research and Ethics Committee (50954615.8.0000.5418/2015). To simulate the clinical oral condition in this *in vitro* study, whole unstimulated human saliva was obtained for 1 h per day over several days from three healthy volunteers (with their informed consent) at least 1.5 h after eating, drinking, or tooth brushing [49].

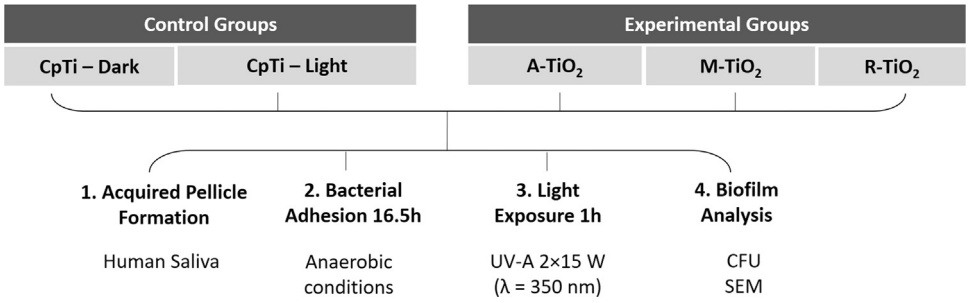

Fig. 2 – Microbiological assay design.

The collected saliva was pooled and centrifuged (30 min, 4 °C, 27,000 g), and the supernatant was pasteurized (60 °C, 30 min) and re-centrifuged in sterile bottles. The supernatant was stored at −20 °C [49]. Prior to acquired pellicle formation, discs were sterilized by gamma radiation (14.50 ± 0.05 kGy) [48]. Each disc was placed in a well of a sterile 24-well polystyrene cell culture plate and incubated with 2 mL of saliva for 4 h at 37 °C [49].

2.5.4. *Biofilm assay*

Strains of *S. sanguinis* IAL 1832, *A. naeslundii* OMZ 745 and *F. nucleatum* OMZ 596 were grown on Columbia blood agar plates supplemented with 5% defibrinated blood sheep (CBA) under anaerobic incubation at 37 °C for 48 h. Loopfuls of CBA-grown colonies were inoculated into 9 mL of filter-sterilized fluid universal medium [50] supplemented with 67 mmol/L Sorensen's buffer, pH 7.2 ("modified fluid universal medium", mFUM) [49] and incubated anaerobically at 37 °C for 24 h. Next, 1 mL from each tube was transferred to a new tube containing 15 mL of mFUM and incubated at 37 °C for 7 h. Then, the optical density of each culture was independently adjusted to OD_{550} 1.00 ± 0.02 and a mixture of all strains was prepared with equal volumes of each density-adjusted culture.

The pellicle-coated discs were transferred to a new 24 well culture plate containing 1.8 mL of medium mixture of saliva (60%), mFUM (30%), horse serum (10%) and 225 μL of mixture-species inoculum. The 24-well polystyrene cell culture plate was incubated anaerobically at 37 °C for 16.5 h [49,51]. After 16.5 h of bacterial adhesion and organization of an early biofilm, discs were washed two times in saline solution (NaCl 0.9%) and transferred to wells containing 2 mL of NaCl 0.9% [52]. The 24-well polystyrene cell culture plate was exposed to UV-A light irradiation for 1 h under the same conditions as of the photocatalytic test and in microaerophilic conditions due to the presence of *F. nucleatum* (anaerobic bacteria). For control, another group of cpTi discs (control surface) was submitted to the same conditions, but in the dark (foil wrapped).

2.6. *Biofilm analysis*

2.6.1. *Colony forming units (CFU)*

The discs were transferred to cryogenic tubes containing 3 mL of NaCl 0.9%, where they were sonicated (7 W for 30 s) to detach cells from the surface. From this cell suspension, an aliquot of 0.1 mL was 7-fold serially diluted in NaCl 0.9% and plated in the following culture medias: Columbia Blood Agar (CBA) supplemented with 5% (v/v) defibrinated blood sheep for the counts of total microorganism count; CBA supplemented with the antibiotics (CBA Plus) norfloxacin (1 mg/L), erythromycin (1 mg/L) and vancomycin (4 mg/L) for *F. nucleatum*; Mitis Salivarius Agar (MSA) for *S. sanguinis* and Cadmium Sulfate Fluoride Acridine Trypticase Agar (CFAT) for *A. naeslundii*. CBA and CBA Plus plates were incubated anaerobically at 37 °C for 72 h, while CFAT and MSA plates were incubated in an atmosphere of 10% CO_2 at 37 °C for 48 h. After obtaining the counts, data were expressed as log of colony forming units per cm^2 (log CFU/cm^2).

2.6.2. *Biofilm Organization by scanning electron microscopy (SEM)*

Additional discs were fixed in Karnovsky solution (PBS; pH 7.2), followed by dehydration in a series of ethanol washes (60%, 70%, 80%, 90% solution for 5 min and 100% for 10 min) and were then allowed to dry aseptically. Afterwards, they were gold-sputtered for observing in SEM (JEOL-JSM-5600LV) scanned at 15 kV at 500× and 5000× magnification [53].

2.7. *Statistical analysis*

One-way ANOVA was used to test the influence of TiO_2 on the surface properties and number of CFU. Two-way repeated measure ANOVA was used to verify the influence of surface

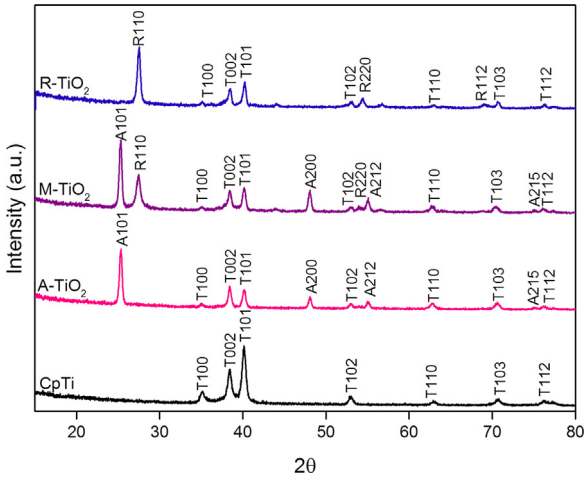

Fig. 3 – X-ray diffraction pattern of CpTi, A-TiO_2, M-TiO_2 and R-TiO_2. The letters T, A and R refers to corresponding peaks of titanium, anatase and rutile, respectively.

treatment and time on the photocatalytic activity of TiO_2. Tukey HSD and Bonferroni tests were used as post hoc techniques for multiple-comparisons when necessary. A mean difference significant at the 0.05 level was used for all tests (IBM Corp. Released 2012. IBM SPSS Statistics for Windows, Version 21.0) and final graphs were done using GraphPad Prism version 4.00 for Windows, GraphPad Software.

3. Results

3.1. *Surface characteristics*

Fig. 3 shows the X-ray diffraction patterns of the cpTi and TiO_2 films. The shape of the diffraction peaks reveals that they are attributed to titanium (T), anatase (A) or rutile (R) phases, with the titanium crystalline phase referring to the substrate. It is important to highlight that the different samples presented different crystalline phases: anatase, mixture (anatase + rutile) and rutile, suggesting that the cpTi discs were successfully coated with TiO_2 films with different crystalline structures.

The morphology of the cpTi substrate and TiO_2 films formed by magnetron sputtering clearly show different surface topographies between cpTi and TiO_2 surfaces (Fig. 4). Cutting marks from the polishing process are noticeably visible on the cpTi surface and, even after the sputtering treatment, these marks are still present (Fig. 4), due to the compact thickness of TiO_2 films, which ranged from 312 to 338 nm (Table 2). Fig. 4a shows that TiO_2 films presented rounded particles smaller than 1 μm and arranged in agglomerates, which is common in TiO_2 nanoparticles [14]. However, no specific orientation was noticeable for any of the three tested surfaces. Fig. 4b shows the two- and three-dimensional profiles of the surfaces. A-TiO_2 and M-TiO_2 surfaces presented greater TiO_2 coverage compared to R-TiO_2, where fewer particles were present (Fig. 4b). When observing the 3D profile, A-TiO_2 presented the greater Ra value followed by R-TiO_2, M-TiO_2 and cpTi. Different average areas were also noted, where

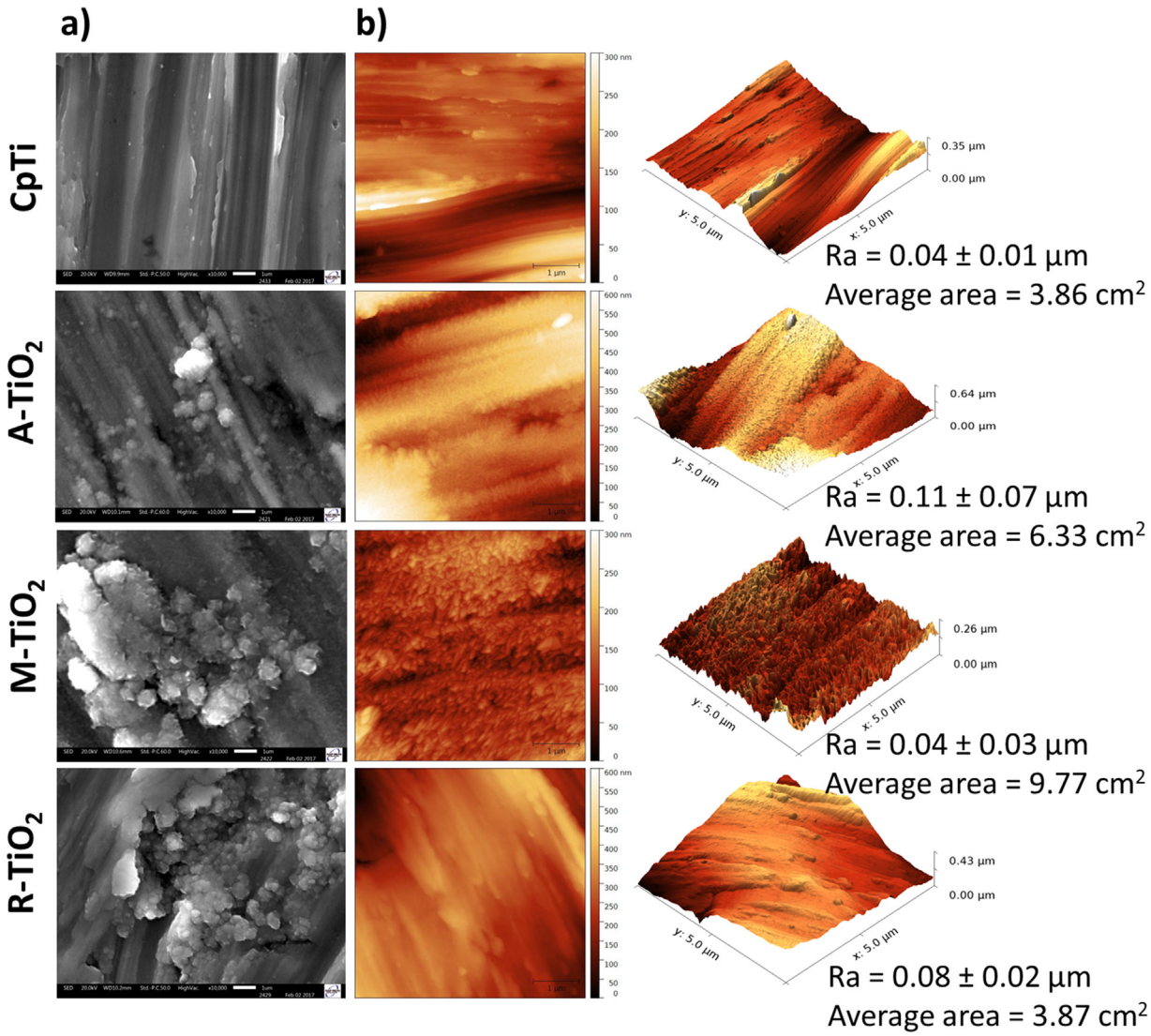

Fig. 4 – Morphology and topography analysis of CpTi, A-TiO_2, M-TiO_2 and R-TiO_2. (a) Secondary electrons SEM micrographs obtained in a 10 mm work distance, at 10,000× magnification and 20 kV electron beam (scale bar = 1 μm) and (b) AFM micrographs obtained in a tapping mode with a constant force 42 N/m and frequency 320 kHz (scale bar = 1 μm).

Table 2 – Results of elemental chemical composition, thickness measurement of TiO_2 films, hardness, elastic modulus and surface free energy of the surfaces. Data are expressed as mean ± standard deviation.

Parameters	Groups			
	CpTi	A-TiO_2	M-TiO_2	R-TiO_2
Elemental composition (at%)				
Carbon	6.31 ± 1.02^{a}	2.68 ± 0.79^{b}	2.21 ± 1.12^{b}	2.10 ± 0.89^{b}
Oxygen	3.89 ± 0.93^{b}	57.07 ± 1.00^{a}	59.35 ± 0.99^{a}	59.88 ± 0.68^{a}
Titanium	89.87 ± 0.06^{a}	40.25 ± 0.98^{b}	38.44 ± 0.87^{b}	38.03 ± 0.77^{b}
Thickness (nm)	–	338 ± 43^{a}	314 ± 16^{a}	312 ± 14^{a}
Hardness (GPa)	4.00 ± 0.26^{d}	5.00 ± 0.71^{c}	7.00 ± 0.85^{b}	9.00 ± 1.14^{a}
Elastic modulus (GPa)	102 ± 4^{b}	89 ± 6^{b}	122 ± 6^{a}	126 ± 24^{a}
Surface free energy (mN/m)				
Polar	8.91 ± 0.01^{a}	4.63 ± 0.01^{b}	4.72 ± 0.04^{b}	3.50 ± 0.01^{b}
Dispersive	36.06 ± 0.03^{ab}	38.94 ± 0.02^{a}	37.83 ± 0.01^{ab}	32.97 ± 0.06^{b}
Total	44.97 ± 0.03^{a}	43.57 ± 0.02^{a}	42.56 ± 0.01^{a}	36.47 ± 0.04^{b}

Different letters indicate significant differences among groups for each dependent variable ($p < 0.05$, Tukey HSD test).

M-TiO_2 revealed greater area followed by A-TiO_2, R-TiO_2 and cpTi (Fig. 4b).

All surfaces presented chemical composition consisting of titanium (Ti), oxygen (O) and carbon (C). The TiO_2 groups presented higher amounts of O and lower content of C and Ti when compared to the control, indicating an oxide film (Table 2).

The TiO_2 films increased the cpTi hardness and the rutile phase presented the greatest values followed by mixture, anatase and cpTi (Table 2). The elastic modulus was also higher in mixture and rutile phases compared to cpTi and anatase phase.

The surface free energy of the studied TiO_2 films was determined as the sum of the dispersive and polar components of the contact angle (Table 2). CpTi, anatase and mixture surfaces presented a similar performance, whereas rutile presented the lowest wettability. This property was measured by contact

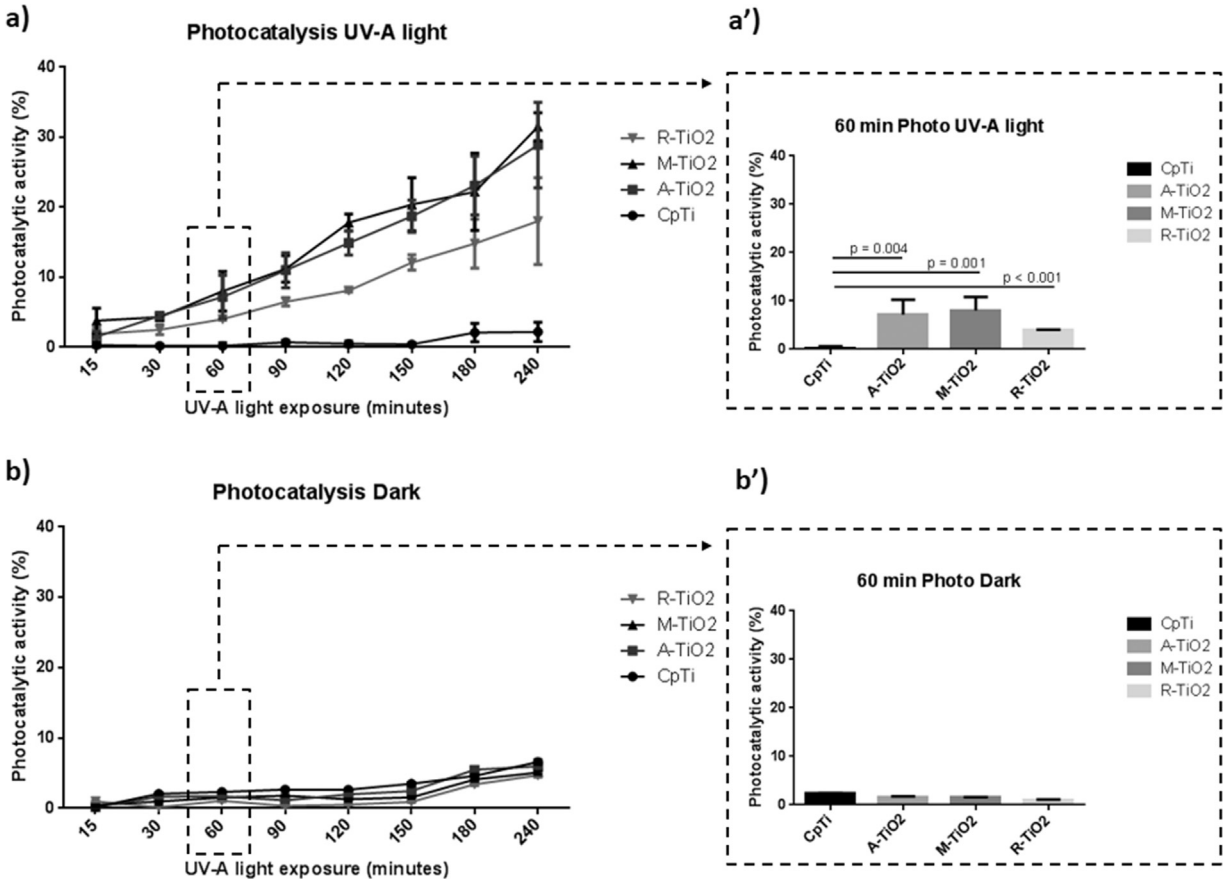

Fig. 5 – Photocatalytic activity of CpTi, A-TiO_2, M-TiO_2 and R-TiO_2 according to the time of UV-A light exposure (a) or dark condition (b), and after 60 min of UV-A light exposure (a') or dark condition (b'). The bars indicate statistical differences between groups ($p < 0.005$).

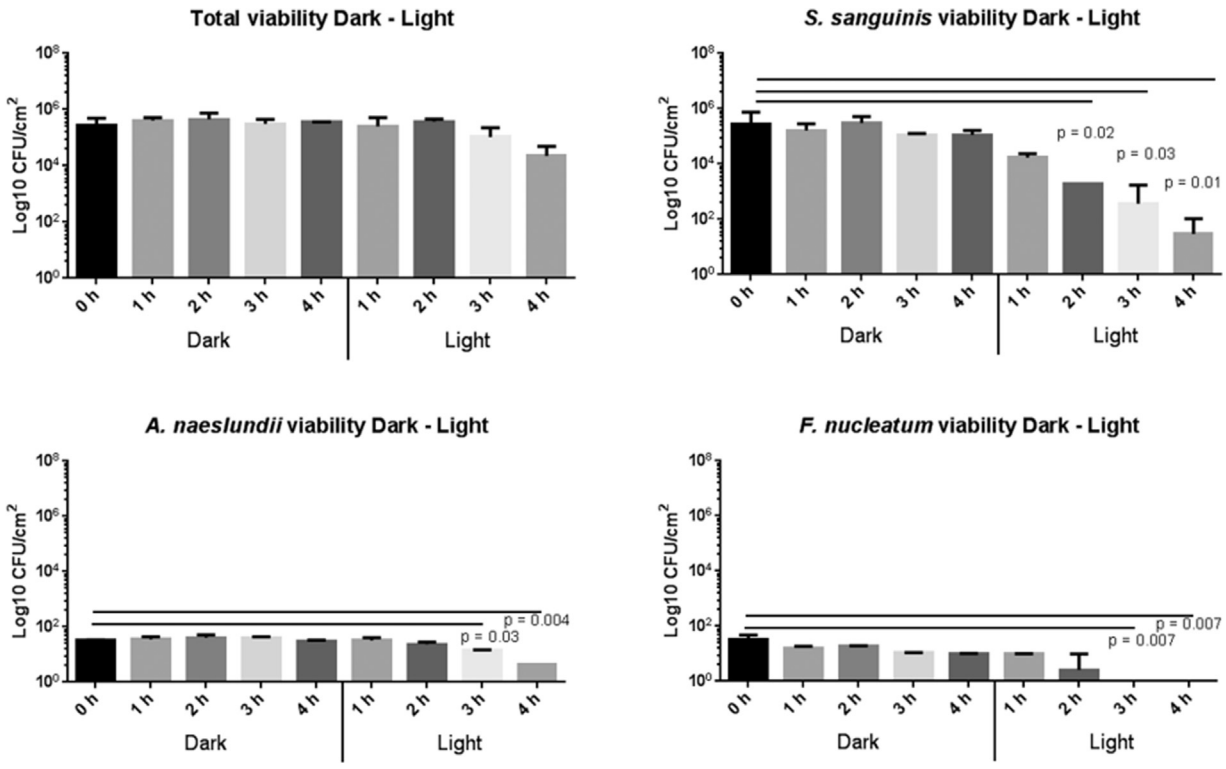

Fig. 6 – Viability of bacteria cells after different UV-A exposure times or dark times on CpTi surfaces. The bars indicate statistical differences between groups ($p < 0.05$; Tukey HSD test).

angle in which a low contact angle suggests a high surface free energy and consequently an improved wettability. The water contact angle measured on CpTi ($\theta = 81°$), anatase ($\theta = 90°$) and mixture ($\theta = 90°$) showed an intermediate hydrophilicity of the surfaces while rutile ($\theta = 95°$) tended towards hydrophobicity.

3.2. *Photocatalytic degradation activity*

The photocatalytic activities of the TiO_2 films were evaluated in the presence of UV-A light and in dark conditions, based on the methylene blue (MB) dye degradation as a function of time. According to the data showed in Fig. 5a, TiO_2 films presented a photocatalytic activity in light that increased over time. Anatase and mixture films showed similar and higher activity compared to the rutile phase and control.

No photocatalytic activity of TiO_2 in dark conditions was noted (Fig. 5b), justifying the non-inclusion of TiO_2 surfaces in dark conditions during the biofilm assay. This was our negative control, showing that TiO_2 films need to be photocatalyzed in order to produce MB degradation. The CpTi surface did not present any significant photocatalytic activity in both conditions, as expected (Fig. 5a,b).

We showed that exposure to UV-A light increased photocatalytic performance for the TiO_2 films proportionally to the time. However, it was necessary to check how bacterial cells could be affected after the UV-A light exposure using control surfaces (CpTi) without TiO_2 films, to avoid confusing dead cell as results of UV-A light instead of the surface treatments. This is important because UV-A damage occurs following the excitation of photosensitive molecules within the cell resulting in physiological alterations, growth delay and oxidative disturbances of bacterial membranes resulting in growth inhibition [54,55].

Thus, by observing the total biofilm viability (Fig. 6), UV-A light did not present significant antibacterial effect on the total CFU counts, even after 4 h of exposure. It leads us to confirm that the UV-A light did not have an antibacterial effect on our multispecies biofilm. However, bacterial CFU counting for each microorganism, separately, showed that after 2 h of UV-A light exposure, antibacterial effect was noticed for *S. sanguinis* and, after 3 h of UV-A light exposure, antibacterial effect was noticed for *A. naeslundii* and *F. nucleatum*. This shows that the use of a single species biofilm might overestimate the effects of UV-A light, showing how important it is to create a biofilm that better resembles *in vivo* complex architecture of oral biofilms. For this reason, it was decided to use 1 h of UV-A light exposure on the subsequent experiments with the TiO_2 films, as this time showed no antibacterial effect on the total viability of our complex multispecies biofilm and on each species alone.

3.3. *Antibacterial action of TiO_2 films*

After 1 h of UV-A light activation A-TiO_2 and M-TiO_2 films presented significant antibacterial effect on multispecies biofilm ($p < 0.001$) with a reduction about 99% and 99.9% of bacterial counts, respectively (Fig. 7). R-TiO_2 films had no antibacterial effect on multispecies biofilm ($p > 0.05$).

By observing SEM images, we could identify images suggestive of *F. nucleatum* or *A. naeslundii* (arrows) and *S. sanguinis* arranged as multicellular aggregates (asterisk). The bacterial

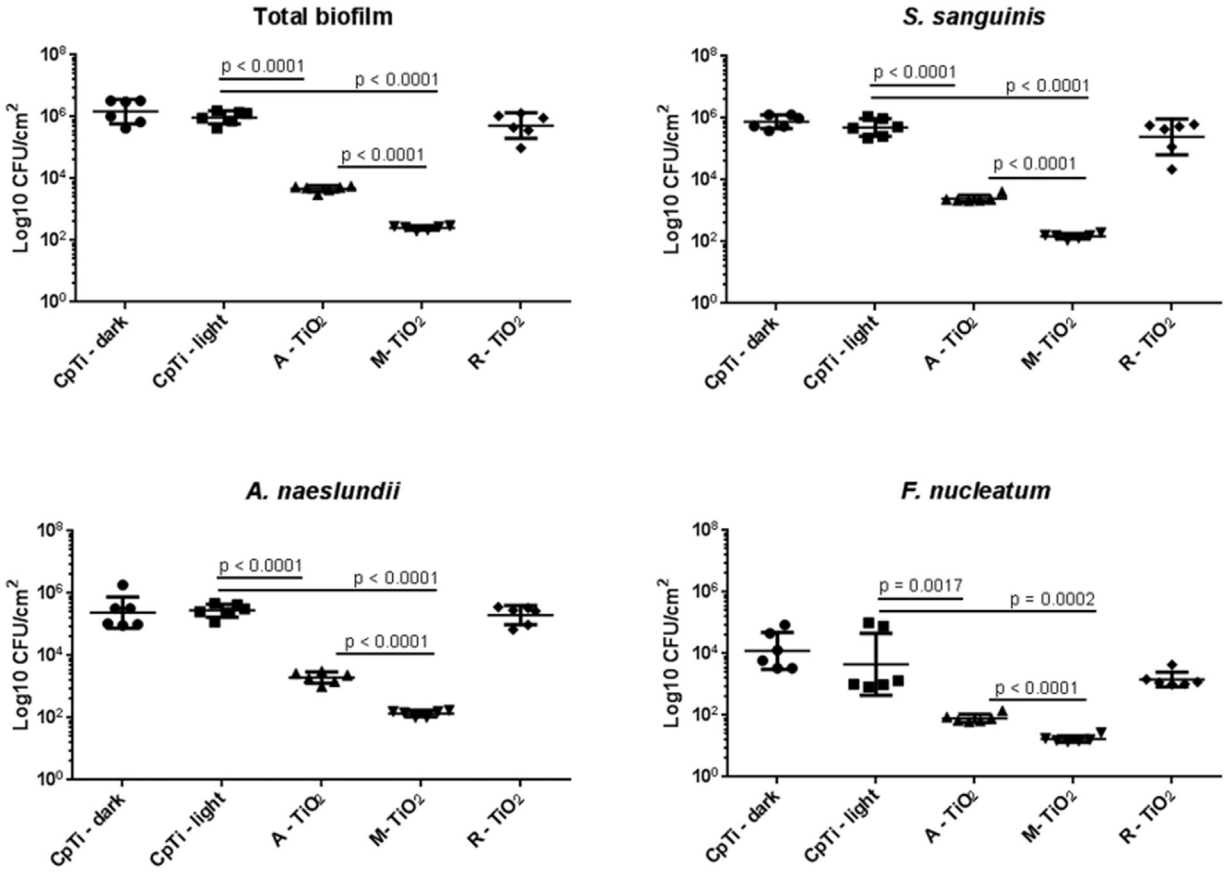

Fig. 7 – Colony forming units (Log_{10} CFU/cm^2) of total number and of each species of microorganisms developed on surfaces after 1 h of UV-A light exposure according to groups. The bars indicate statistical differences between groups ($p < 0.05$; Tukey HSD test). Note: The dark condition was not applied in TiO_2 surfaces since it presented no effect on MB degradation.

reduction observed for A-TiO_2 and M-TiO_2 film was confirmed by SEM (Fig. 8), where images show a thin and disorganized biofilm structure with extended areas of titanium or TiO_2 film not colonized, when comparing to both control titanium groups and the R-TiO_2 group. Details on 5000× magnification show the complex structure still present on controls and R-TiO_2, but absent on both A-TiO_2 and M-TiO_2 film groups.

4. Discussion

Overall, we were capable to develop TiO_2 films with different crystalline phases (anatase, rutile and a mixture of both) onto cpTi surfaces using magnetron sputtering. This led to 300 nm thick films able to improve the hardness and elastic modulus of cpTi surfaces. The UV-A activation of these films generated photocatalytic activity proportionally to the time of exposure and each crystalline phase presented its own antimicrobial effect on the multispecies biofilm tested, therefore our hypothesis that each crystalline phase would have a different antibacterial effect against the *in vitro* biofilm tested was accepted, being M-TiO_2 and A-TiO_2 the best antimicrobial films, eliminating 99.9% and 99% of the multispecies biofilm, respectively.

4.1. *Effect of TiO_2 on the surface properties of cpTi*

All TiO_2 films presented higher hardness compared to cpTi surface in addition to a higher elastic modulus found in mixture and rutile phases. Among them, rutile phase presented the highest values of both hardness and elastic modulus, and it can be attributed to the rutile crystal structure. The higher temperatures during deposition process reflects in the anatase–rutile phase transition enhancing the crystal quality [56], being rutile a more stable phase of TiO_2 [14]. Furthermore, rutile structure is composed by octahedrals connected in its edges, while anatase connects by its vertices, thus rutile presents a denser structure than anatase [57]. This greater mechanical performance of all TiO_2 films compared to cpTi surface is an important finding, since abutments are usually exposed to severe conditions in the oral cavity, such as in biofilm development and abrasive forces during hygiene procedures, such as tooth brushing.

With respect to the biological response to dental implants, the surface wettability is one of the most important parameters influencing the osseointegration process [58]. Hydrophilic surfaces seems to be more favorable to interact with biological fluids, cells and tissues than hydrophobic ones [58]. Rutile (110) presented a hydrophobic tendency, due to its oxygen vacancies which did not lead to the H_2O dissociation on the TiO_2 surface, reflecting on a poor water wetting ability [57].

Furthermore the initial adherence of microorganisms is influenced by the surface roughness of an implant material [59]. However, all surfaces on this study, even after TiO_2 films deposition, presented roughness values lower than 0.2 μm, which is considered a threshold surface roughness for bacterial adhesion, below which biofilm adhesion cannot be reduced further [59].

4.2. *Photocatalytic activity vs. antibacterial effect of TiO_2 films*

The exposure to UV-A light increased photocatalytic performance for the TiO_2 films proportionally to the time. A-TiO_2 and M-TiO_2 films presented the greater photocatalytic activity (Fig. 5), which positively reflected on their higher antibacterial effect. This can be attributed to the presence of anatase phase and its large band gap (3.2 eV) promoting high energy to create electrons and holes, and consequently to form more ROS, when compared to rutile [9,43,48,49].

Although A-TiO_2 and M-TiO_2 presented similar photocatalytic activities ($p = 1.00$) on MB degradation, their antibacterial effects were different ($p < 0.05$). M-TiO_2 presented the greatest antibacterial effect, probably as a result of its robust electron–hole separation and the presence of type II band alignment, which can reduce the recombination of electrons and holes, promoting more ROS [25,60]. Additionally, it is important to highlight that M-TiO_2 revealed a 3 times bigger area than control and 1.5 times bigger area than anatase surface (as previously shown on Fig. 4), which could lead to a higher production of ROS and therefore generating degradation of bacterial membranes in a higher rate than A-TiO_2, thus explaining its higher antibacterial effect [14].

It is interesting to notice that R-TiO_2, which presented the lowest photocatalytic activity, had no antibacterial effect on multispecies biofilm ($p > 0.05$), and even with slightly hydrophobic surface, it still had no effect on biofilm reduction, as it presented CFU counts similar to control groups. This result highlights the directly relation of the photocatalytic activity percentage and the achievement of a significant antibacterial effect. In 1 h of UV-A light, A-TiO_2 presented a photocatalytic activity around 7.2%, M-TiO_2 around 8% and, finally R-TiO_2 presented only 4% (which did not present antibacterial effect). It leads us to conclude that in order to promote significant antibacterial effect, it is necessary a photocatalytic activity percentage above 7%. Furthermore, bacterial adhesion in TiO_2 surfaces without UV-A light activation did not show any

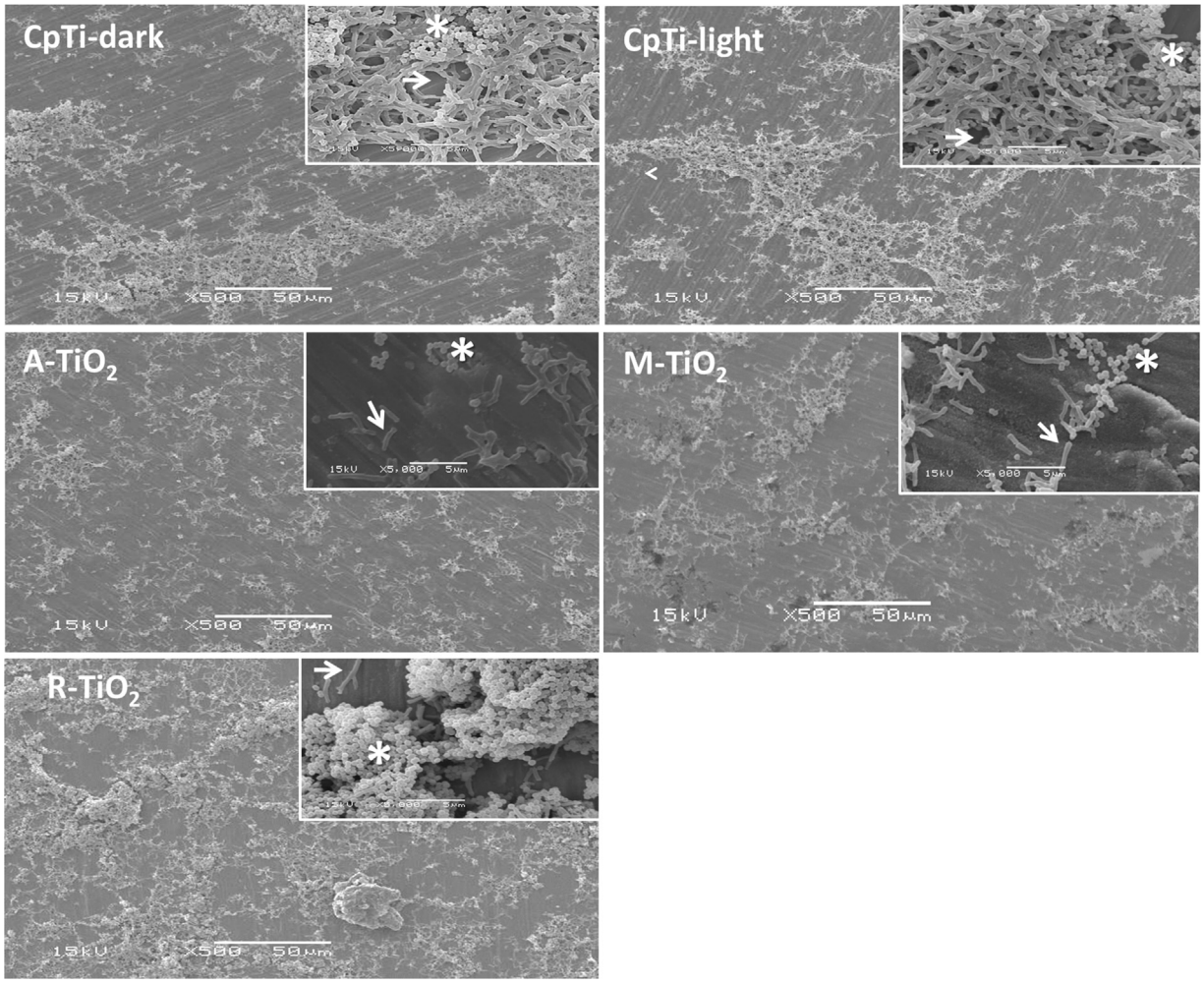

Fig. 8 – SEM micrographs of biofilms formed on CpTi-dark, CpTi-light, A-TiO_2, M-TiO_2 and R-TiO_2 at 500× and 5000× magnification (scale bar = 50 μm). (*) = multicellular aggregates, (arrows) = Spindle-shape rods.

antibacterial effect on *S. sanguinis* and *A. naeslundii* biofilms [36], highlighting the importance of UV-A light activation.

A recent study compared the antibacterial effect of different crystalline phases of TiO_2 pre-treated with UV-A and UV-C lights in a single biofilm of *S. sanguinis* [9]. Even though the moment of light exposure (pre-treatment before biofilm growth) was different than the one used here (after biofilm growth), the results found in this article [9] are in agreement with those found in our study. They showed that the group comprising primarily by anatase phase (UV-A pre-treated) and the mixture of anatase and rutile group (UV-A/UV-C pre-treated), showed a 50% bacterial reduction when compared to control. In our study, the UV-A treatment for 1 h after biofilm formation presented 99.9% bacterial reduction for the mixture of anatase and rutile group and 99% for the anatase phase TiO_2 film. Thus, we believe that these two studies can be considered complementary, where the previous one showed the efficacy of UV exposure before implant insertion, to avoid initial biofilm formation in the initial healing phase right after implant placement [9]; and the current one refers to a post-insertion period of implant, on a late maintenance visit for dental prosthesis cleaning and disinfection, therefore being a promising complementary extra oral hygiene procedure for peri-implant mucositis and peri-implantitis patients.

Even though some other papers have discussed the antimicrobial effect of TiO_2 films [19,20,27,28,39,40], most of them used only one single specie bacteria/fungal for biofilm formation [12,37,38,40,61], which does not completely resemble the oral environment, and as we showed here, could be overestimating the antimicrobial effect, as it used a single specie biofilm model. It is well known that interspecies bacterial interactions and spatially organized biofilms are highly associated with bacterial tolerance to oral antimicrobial products, highlighting the importance of using multispecies biofilms for antimicrobial studies.

Furthermore, this is the first study using the TiO_2 photocatalysis, to show an antibacterial effect on a multispecies biofilm formed over saliva acquired pellicle, which closely resembles the complex biofilm structure found in the oral cavity. Most of the studies did not coated the discs with the acquired pellicle [29–31,40] which seems to have some influence on the TiO_2 photocatalysis effect. Westas et al. studied the influence of acquired pellicle in the TiO_2 antibacterial effect after 24 h of UV light exposure, showing that the TiO_2 antibacterial effect in *Streptococcus oralis* was higher in pellicle coated discs compared to uncoated discs [12]. This can be explained by the fact that UV light is able to promote some decomposition of acquired pellicle layer [11,12,54]. A significantly reduction in adsorbed mass and protein signals and an increase in substrate signals in the pellicle layer were noted in anatase surfaces after UV activation [11]. When using artificial saliva, even in visible light presence (400–410 nm), the pellicle decomposition has been shown [62]. Even though, the period of UV light exposure can lead to pellicle degradation, the UV pre-activation seems to not be harmful to pellicle formation and decomposition in anatase or titanium surfaces [11].

4.3. *Clinical implications, limitations, and future perspectives*

Our results support the antibacterial potential of different crystalline phases of TiO_2 in a relevant model of multispecies bacterial biofilm, formed over saliva acquired pellicle, which closely resembles the complex biofilm structure found in the oral cavity. Rutile-TiO_2 film was the only film that did not present any antibacterial effect on this oral biofilm model, while anatase and mixture-TiO_2 films present a statistically significant biofilm reduction, being able to reduce all 3 species present in this multispecies biofilm.

Although TiO_2 film was not able to completely eliminate the multispecies biofilm formed on the titanium surface, anatase and mixture treatments showed a more porous and disorganized biofilm structure, these TiO_2 surfaces present extended areas without biofilm coverage and no tridimensional colony structure, as observed for control groups and rutile. Clinically this would mean that during a maintenance visit where the prosthesis is removed for cleaning, while the dentist works on the patients mouth, the prosthesis can be under UV-A exposure for 1 h, and after that the remaining biofilm could be easily removed by other oral hygiene procedures, such as brushing, or debridement procedures using plastic instruments, or air abrasive system and rubber cups, which has been previously showed to left the anatase surfaces intact [63]. Thus, considering that the elimination of the biofilm from the implant surface is the prime objective when treating peri-implant mucositis [64], TiO_2 could be a promising complementary method for biofilm control, especially in hard to reach areas in the prostheses.

Even though promising, results gathered in this laboratory are preliminary and therefore should not be immediately transferred to a clinical setting. Although the UV-A is the least harmful type of the UV light [23], it is still harmful to the patient's tissues and cells [23,55,62]. For this reason, results obtained from studies using longer UV-A exposure times, such as 24 h [12,29–31], would not be able to be applied in the patient's oral cavity.

In our study, sputtered anatase and mixture-TiO_2 films promoted at least 99% CFU reduction within only 1 h of UV-A light and >7% photocatalytic degradation activity, which is a great improvement when compared to 24 h exposure from previous studies, but still not clinically acceptable. For this reason, we suggest that the UV-A light can be applied straight to the implant components attached to the prosthesis out of the patient's mouth before placement, or after removal during maintenance and cleaning visits.

Additionally, the findings and methodology developed on this study can help to change the bandgap of TiO_2 and enable its activation by a visible light in the future [13], as long as a minimum of 7% photocatalytic degradation activity is achieved, as this seems to be our threshold percentage to achieve significant antibacterial effect. In this context, we hope that this percentage can soon be achieved with longer wavelengths, in order to still generate photocatalytic attack of biofilms, but also enhance the clinical acceptance of this treatment, extending its use for intra oral areas. This was recently

highlighted by other authors, as an area of great interest in the field of implantology [65].

Moreover, because there is still considerable variability in the test conditions used in previous studies, as it has been highlighted by previous authors [35], it would be useful for future studies to have a standardized methodology as we used here, and for that, we propose the following steps: (1) Establish the accurate light exposure time, light intensity, wave length and light distance to promote the greatest antibacterial effect (through Methylene blue degradation test); (2) Promote the human acquired pellicle formation prior to bacterial adhesion, simulating the oral cavity condition; (3) Perform the tests in a multispecies biofilm which are known to better resembles the *in vivo* condition and is more resistant to antibacterial therapies due to its complex structure; (4) Verify the viability of cells in light presence, independently if the light type is UV or visible; the viability must be evaluated to avoid confusion if the bacterial death is merely due to the light exposure or if it actually has an antibacterial potential (through cell viability test). Following such steps, a consensus about the best protocol to be applied clinically can be achieved.

5. Conclusions

In summary, the TiO_2 films were successfully developed via radiofrequency magnetron sputtering deposition in different crystalline phases. The anatase and mixture phases showed effective antibacterial activity on the oral multispecies biofilm model, being a promising extra oral technique to reduce biofilm on implant abutments surface. In a nutshell, our findings bring favorable results for the photocatalytic activity of TiO_2 films in oral biofilm-associated disease and new insights on the development of new protocols for the photocatalytic activity of TiO_2 in oral biofilm-associated disease.

Funding

This work was supported by the State of Sao Paulo Research Foundation (FAPESP) (grant numbers 2015/17055-8 and 2016/11470-6), and The Brazilian National Council for Scientific and Technological Development (CNPq) (grant number 442786/2014-0).

Acknowledgements

The authors would like to thank the Electron Microscopy Laboratory (NAP/MEPA — ESALQ/USP), Rafael Parra and Jéssica Gonçalves for their support in the Plasma Technology Lab at Univ Estadual Paulista (UNESP), and the Brazilian Nanotechnology National Laboratory (LNNano) for the AFM facility. OMZ strains were kindly donated by Prof. Bernhard Guggenheim to Prof. Jaime A. Cury, and were stored in the collection at the Biochemistry laboratory, Department of Physiological Science at UNICAMP.

REFERENCES

[1] Claffey N, Clarke E, Polyzois I, Renvert S. Surgical treatment of peri-implantitis. J Clin Periodontol 2008;35:316–32, http://dx.doi.org/10.1111/j.1600-051X.2008.01277.x.

[2] Heitz-Mayfield LJ, Mombelli A. The therapy of peri-implantitis: a systematic review. Int J Oral Maxillofac Implants 2014;29(Suppl):325–45, http://dx.doi.org/10.11607/jomi.2014suppl.g5.3.

[3] Derks J, Tomasi C. Peri-implant health and disease. A systematic review of current epidemiology. J Clin Periodontol 2015;42:S158–71, http://dx.doi.org/10.1111/jcpe.12334.

[4] Fürst MM, Salvi GE, Lang NP, Persson GR. Bacterial colonization immediately after installation on oral titanium implants. Clin Oral Implants Res 2007;18:501–8, http://dx.doi.org/10.1111/j.1600-0501.2007.01381.x.

[5] Diaz PI. Microbial diversity and interactions in subgingival biofilm communities. Front Oral Biol 2012;15:17–40, http://dx.doi.org/10.1159/000329669.

[6] Paster BJ, Boches SK, Galvin JL, Ericson E, Lau CN, Levanos VA, et al. Bacterial diversity in human subgingival plaque. J Bacteriol 2001;183:3770–83, http://dx.doi.org/10.1128/JB.183.12.3770.

[7] Teughels W, Van Assche N, Sliepen I, Quirynen M. Effect of material characteristics and/or surface topography on biofilm development. Clin Oral Implants Res 2006;17:68–81, http://dx.doi.org/10.1111/j.1600-0501.2006.01353.x.

[8] Dorkhan M, Hall J, Uvdal P, Sandell A, Svensäter G, Davies JR. Crystalline anatase-rich titanium can reduce adherence of oral streptococci. Biofouling 2014;30:751–9, http://dx.doi.org/10.1080/08927014.2014.922962.

[9] Jain S, Williamson RS, Marquart M, Janorkar AV, Griggs JA, Roach MD. Photofunctionalization of anodized titanium surfaces using UVA or UVC light and its effects against Streptococcus sanguinis. J Biomed Mater Res B Appl Biomater 2017:1–11, http://dx.doi.org/10.1002/jbm.b.34033.

[10] Beltrán-Partida E, Valdez-Salas B, Curiel-Álvarez M, Castillo-Uribe S, Escamilla A, Nedev N. Enhanced antifungal activity by disinfected titanium dioxide nanotubes via reduced nano-adhesion bonds. Mater Sci Eng C 2017;76:59–65, http://dx.doi.org/10.1016/j.msec.2017.02.153.

[11] Rupp F, Haupt M, Eichler M, Doering C, Klostermann H, Scheideler L, et al. Formation and photocatalytic decomposition of a pellicle on anatase surfaces. J Dent Res 2012;91:104–9, http://dx.doi.org/10.1177/0022034511424901.

[12] Westas E, Hayashi M, Cecchinato F, Wennerberg A, Andersson M, Jimbo R, et al. Bactericidal effect of photocatalytically-active nanostructured TiO_2 surfaces on biofilms of the early oral colonizer, *Streptococcus oralis*. J Biomed Mater Res A 2017;105:2321–8, http://dx.doi.org/10.1002/jbm.a.36086.

[13] Wu Y, Klostermann H, Geis-Gerstorfer J, Scheideler L, Rupp F. Photocatalytic effects of reactively sputtered N-doped anatase upon irradiation at UV-A and UV-A/VIS threshold wavelengths. Surf Coatings Technol 2015;272:337–42, http://dx.doi.org/10.1016/j.surfcoat.2015.03.045.

[14] Carp O, Huisman CL, Reller A. Photoinduced reactivity of titanium dioxide. Prog Solid State Chem 2004;32:33–177, http://dx.doi.org/10.1016/j.progsolidstchem.2004.08.001.

[15] Joost U, Juganson K, Visnapuu M, Mortimer M, Kahru A, Nõmmiste E, et al. Photocatalytic antibacterial activity of nano-TiO_2 (anatase)-based thin films: effects on *Escherichia coli* cells and fatty acids. J Photochem Photobiol B Biol 2015;142:178–85, http://dx.doi.org/10.1016/j.jphotobiol.2014.12.010.

[16] Loncar E, Radeka M, Petrovic S, Skapin A, Rudic O, Ranogajec J. Determination of the photocatalytic activity of TiO_2

coatings on clay roofing tile substrates methylene blue as model pollutant. Acta Period Technol 2009;220:125–33, http://dx.doi.org/10.2298/APT0940125L.
[17] Landmann M, Rauls E, Schmidt WG. The electronic structure and optical response of rutile, anatase and brookite TiO_2. J Phys Condens Matter 2012;24, http://dx.doi.org/10.1088/0953-8984/24/19/195503, 195503.
[18] Di Valentin C, Finazzi E, Pacchioni G, Selloni A, Livraghi S, Paganini MC, et al. N-doped TiO_2: theory and experiment. Chem Phys 2007;339:44–56, http://dx.doi.org/10.1016/j.chemphys.2007.07.020.
[19] Choi JY, Chung CJ, Oh KT, Choi YJ, Kim KHK. Photocatalytic antibacterial effect of TiO_2 film of tiag on *Streptococcus mutans*. Angle Orthod 2009;79:528–32, http://dx.doi.org/10.2319/012108-169.1.
[20] Pleskova SN, Golubeva IS, Verevkin YK. Bactericidal activity of titanium dioxide ultraviolet-induced films. Mater Sci Eng C 2016;59:807–17, http://dx.doi.org/10.1016/j.msec.2015.10.021.
[21] Zhuang J, Weng S, Dai W, Liu P, Liu Q. Effects of interface defects on charge transfer and photoinduced properties of TiO_2 bilayer films. J Phys Chem C 2012;2012:2–5.
[22] Kühn KP, Chaberny IF, Massholder K, Stickler M, Benz VW, Sonntag HG, et al. Disinfection of surfaces by photocatalytic oxidation with titanium dioxide and UVA light. Chemosphere 2003;53:71–7, http://dx.doi.org/10.1016/S0045-6535(03)00362-X.
[23] Hockberger PE. A history of ultraviolet photobiology for humans, animals and microorganisms. Photochem Photobiol 2002;76:561–79, http://dx.doi.org/10.1562/0031-8655(2002)076<0561:AHOUPF>2.0.CO;2.
[24] Shalini K, Chandrasekaran S, Shivashankar SA. Growth of nanocrystalline TiO_2 films by MOCVD using a novel precursor. J Cryst Growth 2005;284:388–95, http://dx.doi.org/10.1016/j.jcrysgro.2005.06.053.
[25] Nair RG, Paul S, Samdarshi SK. High UV/visible light activity of mixed phase titania: a generic mechanism. Sol Energy Mater Sol Cells 2011;95:1901–7, http://dx.doi.org/10.1016/j.solmat.2011.02.017.
[26] Joost U, Juganson K, Visnapuu M, Mortimer M, Kahru A, Nõmmiste E, et al. Photocatalytic antibacterial activity of nano-TiO_2 (anatase)-based thin films: effects on *Escherichia coli* cells and fatty acids. J Photochem Photobiol B Biol 2015;142:178–85, http://dx.doi.org/10.1016/j.jphotobiol.2014.12.010.
[27] Liu P, Hao Y, Zhao Y, Yuan Z, Ding Y, Cai K. Surface modification of titanium substrates for enhanced osteogenetic and antibacterial properties. Colloids Surf B Biointerfaces 2017;160:110–6, http://dx.doi.org/10.1016/j.colsurfb.2017.08.044.
[28] Liu L, Bhatia R, Webster T. Atomic layer deposition of nano-TiO_2 thin films with enhanced biocompatibility and antimicrobial activity for orthopedic implants. Int J Nanomed 2017;12:8711–23, http://dx.doi.org/10.2147/IJN.S148065.
[29] Shah AG, Shetty PC, Ramachandra CS, Bhat NS, Laxmikanth SM. In vitro assessment of photocatalytic titanium oxide surface modified stainless steel orthodontic brackets for antiadherent and antibacterial properties against *Lactobacillus acidophilus*. Angle Orthod 2011;81:1028–35, http://dx.doi.org/10.2319/021111-101.1.
[30] Cao S, Liu B, Fan L, Yue Z, Liu B, Cao B. Highly antibacterial activity of N-doped TiO_2 thin films coated on stainless steel brackets under visible light irradiation. Appl Surf Sci 2014;309:119–27, http://dx.doi.org/10.1016/j.apsusc.2014.04.198.
[31] Cao B, Wang Y, Li N, Liu B, Zhang Y. Preparation of an orthodontic bracket coated with an nitrogen-doped TiO_2-xNy thin film and examination of its antimicrobial performance. Dent Mater J 2013;32:311–6, http://dx.doi.org/10.4012/dmj.2012-155.
[32] Lim JC, Song KJ, Park C. The effect of deposition parameters on the phase of TiO_2 films grown by RF magnetron sputtering. J Korean Phys Soc 2014;65:1896–902, http://dx.doi.org/10.3938/jkps.65.1896.
[33] Yaghoubi H, Taghavinia N, Alamdari EK, Volinsky AA. Nanomechanical properties of TiO_2 granular thin films. ACS Appl Mater Interfaces 2010;2:2629–36, http://dx.doi.org/10.1021/am100455q.
[34] Mráz S, Schneider JM. Structure evolution of magnetron sputtered TiO_2 thin films. J Appl Phys 2011;10:109, http://dx.doi.org/10.1063/1.3536635.
[35] Hickok NJ, Shapiro IM, Chen AF. The impact of incorporating antimicrobials into implant surfaces. J Dent Res 2017, http://dx.doi.org/10.1177/0022034517731768, 2203451773176.
[36] Frojd V, Linderbäck P, Wennerberg A, Chávez de Paz L, Svensäter G, Davies JR. Effect of nanoporous TiO_2 coating and anodized Ca^{2+} modification of titanium surfaces on early microbial biofilm formation. BMC Oral Health 2011;11:8, http://dx.doi.org/10.1186/1472-6831-11-8.
[37] Jia L, Qiu J, Du L, Li Z, Liu H, Ge S. TiO_2 nanorod arrays as a photocatalytic coating enhanced antifungal and antibacterial efficiency of Ti substrates. Nanomedicine 2017;12, http://dx.doi.org/10.2217/nnm-2016-0398, nnm-2016-0398.
[38] Totu EE, Nechifor AC, Nechifor G, Aboul-Enein HY, Cristache CM. Poly(methyl methacrylate) with TiO2nanoparticles inclusion for stereolitographic complete denture manufacturing—the fututre in dental care for elderly edentulous patients? J Dent 2017;59:68–77, http://dx.doi.org/10.1016/j.jdent.2017.02.012.
[39] Joost U, Juganson K, Visnapuu M, Mortimer M, Kahru A, Nõmmiste E, et al. Photocatalytic antibacterial activity of nano-TiO_2 (anatase)-based thin films: effects on *Escherichia coli* cells and fatty acids. J Photochem Photobiol B 2015;142:178–85, http://dx.doi.org/10.1016/j.jphotobiol.2014.12.010.
[40] Shiraishi K, Koseki H, Tsurumoto T, Baba K, Naito M, Nakayama K, et al. Antibacterial metal implant with a TiO_2-conferred photocatalytic bactericidal effect against *Staphylococcus aureus*. Surf Interface Anal 2009;41:17–22, http://dx.doi.org/10.1002/sia.2965.
[41] Barão VAR, Mathew MT, Assunção WG, Yuan JCC, Wimmer MA, Sukotjo C. Stability of cp-Ti and Ti-6Al-4V alloy for dental implants as a function of saliva pH—an electrochemical study. Clin Oral Implants Res 2012;23:1055–62, http://dx.doi.org/10.1111/j.1600-0501.2011.02265.x.
[42] Pereira ALJ, Gracia L, Beltrán A, Lisboa-Filho PN, Da Silva JHD, Andrés J. Structural and electronic effects of incorporating Mn in TiO_2 films grown by sputtering: anatase versus rutile. J Phys Chem C 2012;116:8753–62, http://dx.doi.org/10.1021/jp210682d.
[43] Cisneros JI. Optical characterization of dielectric and semiconductor thin films by use of transmission data. Appl Opt 1998;37:5262–70, http://dx.doi.org/10.1364/AO.37.005262.
[44] Matos AO, Ricomini-Filho AP, Beline T, Ogawa ES, Oliveira BEC, de Almeida AB, et al. Three-species biofilm model onto plasma-treated titanium implant surface. Colloids Surfaces B Biointerfaces 2017;152:354–66, http://dx.doi.org/10.1016/j.colsurfb.2017.01.035.
[45] Santos DCR, Mota RP, Honda RY, Cruz NC, Rangel EC. Plasma-polymerized acetylene nanofilms modified by nitrogen ion implantation. Appl Surf Sci 2013;275:88–93, http://dx.doi.org/10.1016/j.apsusc.2013.01.105.

[46] Combe EC, Owen BA, Hodges JS. A protocol for determining the surface free energy of dental materials. Dent Mater 2004;20:262–8, http://dx.doi.org/10.1016/S0109-5641(03)00102-7.
[47] Mills A. An overview of the methylene blue ISO test for assessing the activities of photocatalytic films. Appl Catal B Environ 2012;128:144–9, http://dx.doi.org/10.1016/j.apcatb.2012.01.019.
[48] Soriano I, Martín AY, Évora C, Sánchez E. Biodegradable implantable fluconazole delivery rods designed for the treatment of fungal osteomyelitis: influence of gamma sterilization. J Biomed Mater Res A 2006;77A:632–8, http://dx.doi.org/10.1002/jbm.a.30657.
[49] Guggenheim B, Giertsen E, Schüpbach P, Shapiro S. Validation of an in vitro biofilm model of supragingival plaque. J Dent Res 2001;80:363–70, http://dx.doi.org/10.1177/00220345010800011201.
[50] Gmur R, Guggenheim B. Antigenic heterogeneity of *Bacteroides intermedius* as recognized by monoclonal antibodies. Infect Immun 1983;42:459–70.
[51] Guggenheim B, Meier A. In vitro effect of chlorhexidine mouth rinses on polyspecies biofilms. Schweiz Monatsschr Zahnmed 2011;121:432–41.
[52] Cushnie TPT, Robertson PKJ, Officer S, Pollard PM, McCullagh C, Robertson JMC. Variables to be considered when assessing the photocatalytic destruction of bacterial pathogens. Chemosphere 2009;74:1374–8, http://dx.doi.org/10.1016/j.chemosphere.2008.11.012.
[53] de Lucena-Ferreira SC, Ricomini-Filho AP, da Silva WJ, Cury JA, Del Bel Cury AA. Influence of daily immersion in denture cleanser on multispecies biofilm. Clin Oral Investig 2014;18:2179–85, http://dx.doi.org/10.1007/s00784-014-1210-9.
[54] Pizarro RA, Orce LV. Membrane damage and recovery associated with growth delay induced by near-UV radiation in Escherichia coli K-12. Photochem Photobiol 1988;47:391–7, http://dx.doi.org/10.1111/j.1751-1097.1988 tb02742. x.
[55] Robertson JMC, Robertson PKJ, Lawton LA. A comparison of the effectiveness of TiO_2 photocatalysis and UVA photolysis for the destruction of three pathogenic micro-organisms. J Photochem Photobiol A Chem 2005;175:51–6, http://dx.doi.org/10.1016/j.jphotochem.2005.04.033.
[56] Heo CH, Lee S-B, Boo J-H. Deposition of TiO_2 thin films using RF magnetron sputtering method and study of their surface characteristics. Thin Solid Films 2005;475:183–8, http://dx.doi.org/10.1016/j.tsf.2004.08.033.
[57] Diebold U. The surface science of titanium dioxide. Surf Sci Rep 2003;48:53–229, http://dx.doi.org/10.1016/S0167-5729(02)00100-0.
[58] Escada AL, Nakazato RZ, APRA Claro, Escada AL, Nakazato RZ, Claro APRA. Influence of anodization parameters in the TiO_2 nanotubes formation on Ti-7.5Mo alloy surface for biomedical application. Mater Res 2017;20:1282–90, http://dx.doi.org/10.1590/1980-5373-mr-2016-0520.
[59] Bollen CM, Lambrechts P, Quirynen M. Comparison of surface roughness of oral hard materials to the threshold surface roughness for bacterial plaque retention: a review of the literature. Dent Mater 1997;13:258–69.
[60] Scanlon DO, Dunnill CW, Buckeridge J, Shevlin SA, Logsdail AJ, Woodley SM, et al. Band alignment of rutile and anatase TiO_2. Nat Mater 2013;12:798–801, http://dx.doi.org/10.1038/nmat3697.
[61] Valdez-Salas B, Beltrán-Partida E, Castillo-Uribe S, Curiel-Álvarez M, Zlatev R, Stoytcheva M, et al. In vitro assessment of early bacterial activity on micro/nanostructured Ti6Al4V surfaces. Molecules 2017;22:1–16, http://dx.doi.org/10.3390/molecules22050832.
[62] Wu Y, Geis-Gerstorfer J, Scheideler L, Rupp F. Photocatalytic antibacterial effects on TiO_2-anatase upon UV-A and UV-A/VIS threshold irradiation. Biofouling 2016;32:583–95, http://dx.doi.org/10.1080/08927014.2016.1170118.
[63] Kister F, Specht O, Warkentin M, Geis-Gerstorfer J, Rupp F. Peri-implantitis cleaning instrumentation influences the integrity of photoactive nanocoatings. Dent Mater 2017;33:e69–78, http://dx.doi.org/10.1016/j.dental.2016.10.002.
[64] Heitz-Mayfield L, Needleman I, Salvi G, Pjetursson B. Consensus statements and clinical recommendations for prevention and management of biologic and technical implant complications. Int J Oral Maxillofac Implants 2014;29:346–50, http://dx.doi.org/10.11607/jomi.2013.g5.
[65] Rupp F, Liang L, Geis-gerstorfer J, Scheideler L, Hüttig F. Surface characteristics of dental implants: a review. Dent Mater 2018;34:40–57, http://dx.doi.org/10.1016/j.dental.2017.09.007.